Desalination and Water Treatment
www.deswater.com

doi: 10.5004/dwt.2023.29741

300 (2023) 120–129
July

Effective adsorption of 2-nitroaniline from wastewater applying mesoporous material MCM-48: equilibrium, isotherm, and mechanism investigation

Alyaa E. Mahdi[a], Nisreen S. Ali[b], Hassan Sh. Majdi[c], Talib M. Albayati[a,*], Mahir A. Abdulrahman[a], Dheyaa. J. Jasim[d,e], Khairi R. Kalash[f], Issam K. Salih[c]

[a]*Department of Chemical Engineering, University of Technology-Iraq, 52 Alsinaa St., P.O. Box: 35010, Baghdad, Iraq, emails: Talib.M.Naieff@uotechnology.edu.iq (T.M. Albayati), Alyaa.E.Mahdi@uotechnology.edu.iq (A.E. Mahdi), mahir.a.abdulrahman@uotechnology.edu.iq (M.A. Abdulrahman)*
[b]*Materials Engineering Department, College of Engineering, Mustansiriyah University, Baghdad, Iraq, email: nisreensabah@uomustansiriyah.edu.iq (N.S. Ali)*
[c]*Department of Chemical Engineering and Petroleum Industries, Al-Mustaqbal University, Babylon 51001, Iraq, emails: hasanshker1@gmail.com (H. Sh. Majdi), Dr_IssamKamil@mustaqbal-college.edu.iq (I.K. Salih)*
[d]*Department of Petroleum Engineering, Al-Amarah University College, Maysan*
[e]*General Company for Food Products, Ministry of Industry and Minerals, Baghdad 10011, Iraq, email: dhyiaa.joumaa@alamarahuc.edu.iq (D.J. Jasim)*
[f]*Environment and Water Directorate, Ministry of Science and Technology, Baghdad, Iraq, email: khairirs@gmail.com (K.R. Kalash)*

Received 6 March 2023; Accepted 28 June 2023

ABSTRACT

In this work, the MCM-48 mesoporous material was prepared and characterized to apply it as an active adsorbent for the adsorption of 2-nitroaniline (2-nitrobenzenamine) from wastewater. The MCM-48 characterizations were specified by implementing various techniques such as scanning electron microscopy, energy-dispersive X-ray analysis, X-ray diffraction, Brunauer–Emmett–Teller surface area, pore-size distribution, and Fourier-transform infrared spectroscopy. The batch adsorption results showed that the MCM-48 was very active for the 2-nitroaniline adsorption from wastewater. The adsorption equilibrium results were analyzed by applying isotherms like Langmuir and Freundlich. The Langmuir isotherm was used to calculate the theoretical and experimental maximal adsorption capacity of 100 and 65 mg/g, respectively. The Langmuir model is superior to the Freundlich model for the adsorption of 2-nitroaniline onto the mesoporous material MCM-48. The results demonstrated that the kinetics models of the adsorption are very fast and close to the pseudo-second-order model. The findings of adsorption isotherms and kinetics studies indicate the adsorption mechanism is a chemisorption and physical adsorption process.

Keywords: Mesoporous material; 2-Nitrobenzenamine; Adsorption isotherm; Adsorption kinetics; Wastewater treatment; Adsorption mechanism; Characterization MCM-48; Preparation MCM-48; Dye removal; Adsorbent regeneration

1. Introduction

In the modern world, numerous organic pollutants, particularly nitro compounds, have become a significant source of water and environmental contamination [1,2]. Industries including those in the food, pharmaceutical, petrochemical, chemical, pulp, electronics, and paper sectors all create enormous amounts of waste discharges with considerable potential for recycling and remediation [3]. In the paint, plastic, pesticide, dye, and intermediate industries of

* Corresponding author.

the chemical industries, 2-nitroaniline ($C_6H_6N_2O_2$) is used as a diazo component in azo dyes and pigments and as an intermediate for vat dyes. [4]. Many serious environmental problems were caused by wastewater containing 2-nitroaniline, because of its carcinogenic properties and high toxicity [5,6]. Some methods such as membrane, advanced oxidation processes, and adsorption have been used to remove nitro anilines from water [7,8]. Membrane systems have alternatives, such as chemically based oxidation processes and air/oxygen-based on non or oxidation. The first class comprises advanced oxidation processes (AOPs), which produce hydroxyl radicals that are then used for oxidation by using hydrogen peroxide, UV light, and ozone [9–12]. The second class consists of wet air, catalytic wet air, and dry oxidation [13–15]. Another type of treatment used in wastewater cleanup is adsorption. Adsorption techniques have been used to eliminate organic and inorganic contaminants from wastewater, with a particular emphasis on the usage of various materials as the preferred adsorbent. It may be said that the regeneration of the used adsorbent materials is a time-consuming and expensive procedure [13]. Because of this, there is interest in creating new adsorbents to remove contamination in the aqueous waste stream [14,15]. Based on the size, shape, and other characteristics of a molecule, such as polarity, zeolites can reject or selectively adsorb certain compounds. This means that they can act as adsorbents. Organ clays have been the focus of several investigations on organic molecule adsorption from aqueous solutions. There have been reports on silicate [16], mesoporous materials [17], modified and unmodified zeolites [18–20]. For application in separation procedures as an adsorbent, the candidate MCM-48 appears to be more promising. Scientists have been very interested in the mesoporous material MCM-48 since it was discovered by Mobil Oil researchers in 1992 because of its potential use as supports of catalyst, catalysts, and absorbents. These material properties are high thermal stability, specific pore volume up to 1.2 cm/g, surface areas (1,000–1,500 m^2/g), a narrow pore-size distribution, and "non-cytotoxic" properties [21]. Mesoporous silica-based materials, including MCM-48, have been developed as efficient catalyst carriers, adsorbents, and cutting-edge drug delivery systems [22]. This is due to their very considerable thermal stabilities, porous morphologies, extremely large surface areas, and highly reactive surfaces for the presence of the silanol groups [23,24].

The main aim of the present research was to investigate the removal of 2-nitroaniline ($C_6H_6N_2O_2$) from wastewater solutions by applying MCM-48 as an efficient adsorbent. The adsorption isotherms and kinetics were examined. Moreover, the adsorption mechanism of 2-nitroaniline wastewater onto the surface of MCM-48 adsorbent was studied in a batch adsorption process. Finally, regeneration and desorption kinetics were also tested for MCM-48 to discover the actual adsorbent utility and its applicability for reusability in a continuous adsorption system.

2. Experimental set-up

2.1. Chemicals

The chemicals applied for this work were cetyltrimethylammonium bromide $C_{19}H_{42}BrN$ (CTAB; purity > 98%) as a surfactant, tetraethyl orthosilicate $Si(OC_2H_5)_4$ (TEOS; purity > 98% (as a silica source, sodium hydroxide (NaOH), hydrochloric acid (HCl), and 2-nitroaniline (2-nitrobenzenamine) ($C_6H_6N_2O_2$). All reactants were analytically purchased from Sigma-Aldrich Chemical Company (Germany). All materials were applied without additional purification.

2.2. Preparation of MCM-48

According to the preparation method outlined by [25–27], MCM-48 was synthesized. The following steps were used to create MCM-48 in a representative preparation: 90 g of deionized water mixed with 10 g of CTAB. 1 g of NaOH was then mixed with the solution after it had been rapidly agitated at 35°C for 40 min. 11 cm^3 of TEOS was added, after stirring the solution for 60 min at 35°C, and the mixture was then stirred at this temperature for another 30 min. Final heating of the combination was place in an autoclave under static conditions for 24 h at 150°C; the resultant MCM-48 was then cooled down for 1 h, filtrated, and rinsed with distilled H_2O before being dry at ambient temperature. The produced sample was then calcined for 6 h at a temperature of 650°C applying a ramp rate for heating 2°C/min.

2.3. Characterization

The MiniFlex (Rigaku) diffractometer was used to record the patterns of small-angle X-ray diffraction (XRD) in ambient settings using Cu K radiation (λ = 1.5406 Å). The X-ray tube was run at 40 kV and 30 mA, and the data were reported in the 2θ range of 0.5°–8° with a 2-step size of 0.01 and a step time of 10 s. The formulae $n\lambda = 2d\sin\theta$ and $a_o = 2d100/\sqrt{3}$ were applied to determine the unit cell and d-spacing characteristics. The pore analyzer of a Micromeritics ASAP 2020 was used to assess the adsorption and desorption of nitrogen using N_2 physisorption at –196°C. All specimens were degassed in the degas adsorption analyzer port for 3 h at 350°C and vacuum ($p < 10^{-5}$ m·bar). The Brunauer–Emmett–Teller (BET) method was used to calculate the specimens' BET-specific surface areas for the relative pressure range of 0.05–0.25. With the use of the Barrett–Joyner–Halenda approach, which is based on thermodynamics, the distributions of pore size were specified from the isotherm desorption branch. The quantity of liquid N_2 adsorbed at P/P_0 = 0.995 was used to calculate the total pore volume. This information was obtained from the N_2 isotherm's adsorption branch. Through the use of the unit cell parameter (a_o) and pore size diameter, the pore walls thickness (t_W) was estimated (d_p). Using BET analysis (4V/A), the average mesopore sizes for the single specimens were calculated from the data of nitrogen sorption. Scanning electron microscopy (SEM) was carried out on a JEOL (JSM-5600LV) (JEOL, Tokyo, Japan). Energy-dispersive X-ray analysis (EDAX) is an analytical method that creates the adsorbent elemental analysis to determine the composition of chemicals when combined with SEM. Using a Nicolet 380 FTIR spectrometer, the solid samples' infrared spectra were measured were in the 4,000–400 cm^{-1} range at areas with 4 cm^{-1} resolution in transmission mode at ambient temperature [28,29].

2.4. Experiments of batch adsorption

To assess 2-nitroaniline isotherms of adsorption onto the adsorbents at 25°C, batch adsorption tests were performed. 2-Nitroaniline stock solutions were created by dissolving 0.2 g in 1 L of distilled H_2O. At 25°C, experiments of batch adsorption were used to assess the 2-nitroaniline adsorption over the adsorbents. By dissolving 0.2 g of 2-nitroaniline in 1 L of distilled water, stock solutions of 2-nitroaniline were created. Then, 10 concentrations (0–0.2 g/L) were used to create a calibration curve using a UV spectrometer (model HP 8453) calibrated to 25°C. λ_{max} was discovered to be 282 nm. The calibration was necessary to compare final absorbance with beginning absorbance. In 100 mL conical flasks, 15 different concentrations of the afore-mentioned solutions were created, starting from 0.001–0.06 g/L. 100 mL of each was added to 0.01 g MCM-48, which was then stirred in several positions at 150 rpm for 1 h at room temperature (25°C). This made it possible for the mesoporous substance MCM-48 to completely mix with the mixture. Following the adsorption procedure, equal quantities of the solutions were centrifuged for 5 min at 3,500 rpm using a centrifuge (model Hermle Z 200 A). This allowed the zeolite to completely separate from the solution and enable analysis with a UV spectrophotometer (TU1900) operating at a wavelength of 282 nm. According to the following equation, the (%*R*) of 2-nitroaniline was calculated [30]:

$$\%R = \frac{C_o - C_e}{C_o} \times 100\% \quad (1)$$

Using the following equation, the amount of adsorption (q_e) was determined [31]:

$$q_e = \frac{V\left(C_o - C_e\right)}{m} \quad (2)$$

where q_e (mg/g) denotes the adsorption amount, V (L) is the 2-nitroaniline solution volume, m (g) is the mass of the absorbent applied used in the experiments, C_o (mg/L) and C_e (mg/L) are the initial and equilibrium concentration of 2-nitroaniline, respectively. Where q_e (mg/g) is the amount of 2-nitroaniline that will be absorbed, V (L) is the volume of the 2-nitroaniline solution, C_o (mg/L) and C_e (mg/L) are the 2-nitroaniline starting and equilibrium concentrations in the liquid phase, and m (g) is the absorbent mass that will be utilized in the experiment [32].

2.5. Adsorbent's reuse

The regeneration was studied applying an exhausted MCM-48 adsorbent. Following the 2-nitroaniline adsorption solutions onto MCM-48, the mixture was filtered, the discarded adsorbent material that had uptake 2-nitroaniline was rinsed in a sizable amount of H_2O until no 2-nitroaniline remained in solution, and then dried under vacuum conditions at 60°C for the duration of an entire night. Several adsorption–desorption cycles were achieved in order to examine the MCM-48 material's resilience and potential for regeneration.

3. Results and discussion

3.1. Synthesized materials characterization

The prepared MCM-48 was subjected to SEM and EDAX characterization procedures. At a magnification of 1000, SEM pictures of this material are displayed in Fig. 1A.

The peaks on the EDAX graph in Fig. 1B show the components' average weight % values that C, O, and Si made up the zeolite. To get accurate average weight % for each of the components, EDAX graphs were created for a number of different locations on the sample surface. The chemical analysis shows that the carbon weight percent in the MCM-48 is 5.29, indicating the inclusion of surfactant counter anions. It was observed that carbon networks were equally formed in the two channels of MCM-48 without changing the space-group symmetry and that the symmetry of Ia3d was retained after the dissolution of silica mesoporous MCM-48 during the calcination.

As can be displayed in Fig. 2, the MCM-48 small angle XRD patterns exhibit a strong mesostructured-descriptive diffraction peak at around 2θ of 0.9°. Furthermore, two further peaks, indexed as (2 1 1), and (2 2 0) were seen in the XRD patterns. Two reflection peaks at 2θ less than 3° and a string of sporadic weak peaks in the range3.5°–5.5° are indexed to the Ia3d cubic structure. When compared

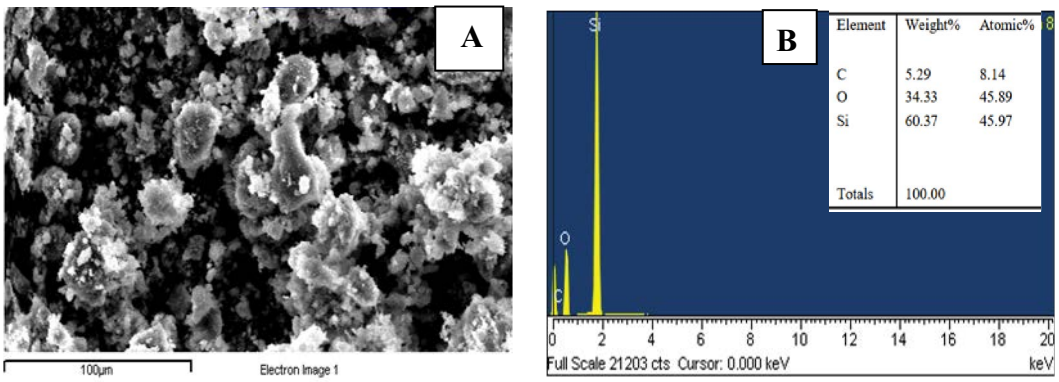

Fig. 1. (A) Scanning electron microscopy picture of MCM-48 at a 1,000x magnification. (B) A typical MCM-48 energy-dispersive X-ray analysis picture.

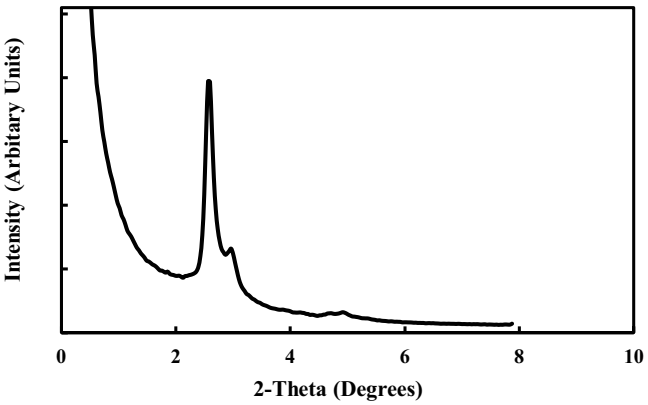

Fig. 2. MCM-48's X-ray diffraction pattern.

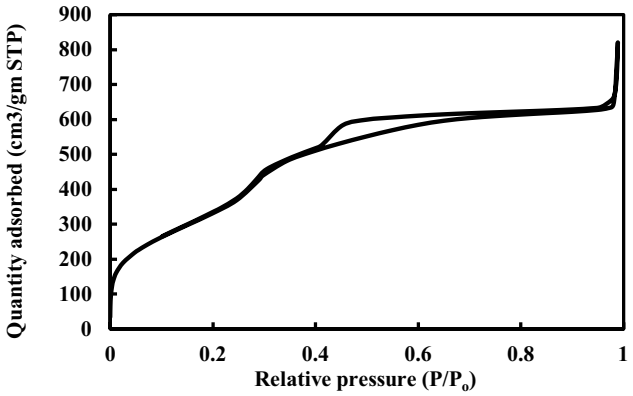

Fig. 3. Isotherms of nitrogen adsorption and desorption for MCM-48.

Table 1
MCM-48's physico-chemical characteristics

Sample	MCM-48
S_{BET} (m^2/g)	1,350
V_P (cm^3/g)	1.4
$V_{\mu P}$ (cm^3/g)	0.6
d_P (nm)	3.3
a_o (nm)	3.6
t_{wall} (nm)	0.7

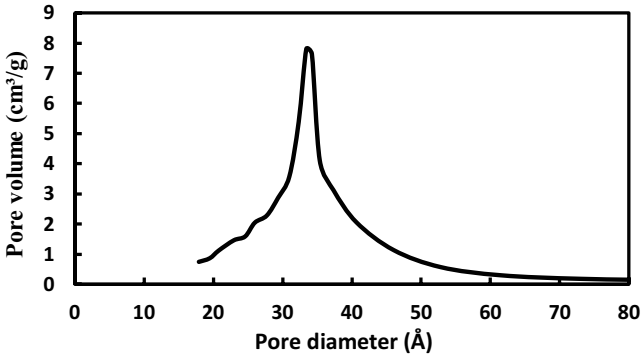

Fig. 4. MCM-48 Barrett–Joyner–Halenda pore-size distribution.

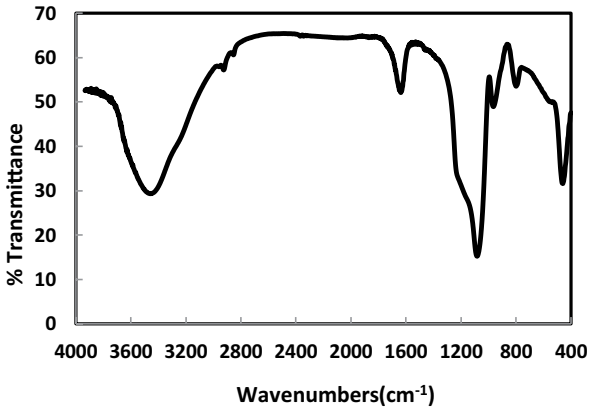

Fig. 5. MCM-48 Fourier-transform infrared spectra.

to comparable peaks described in the literature, the peaks acquired in our investigation match those reported there quite well [33]. The outcomes shown in Table 1 illustrate how MCM-48 has a periodic ordered structure.

According to Fig. 3, the N_2 adsorption isotherms of MCM-48 have a type IV isotherm and a type H1 hysteresis loop. A small pore-size distribution is indicated by sharp adsorption and desorption branches. The sharpness and height of the capillary condensation process in the isotherms, in general, represent the uniformity of the pore size for mesoporous molecular sieves. In the relative pressure (P/P_0) range of 0.05 to 0.25, the MCM-48 displays type IV isotherm, as illustrated in Fig. 3. Together with the structural features discovered by nitrogen adsorption investigations, Table 1 explains the sample's specific surface area, pore size, pore volume, and wall thickness together with the structural characteristics obtained from nitrogen adsorption studies.

Fig. 4 displays the pore-size distribution for the MCM-48. The content produced by CTAB:NaOH. The pore-size distribution of TEOS is broad and centered at 34 Å. A mesopores higher amount was discovered for the basic synthesisation, which created the most evident pore size dispersion and had a fairly regular organization [34].

Fig. 5 displays the Fourier-transform infrared (FTIR) spectrum of MCM-48, which includes the characteristic Si–O–Si bands at 1,082; 964; 799 and 460 cm^{-1}. Stretching vibrations either Si–OH or Si–O–Si can be attributed to the absorption band at around 960 cm^{-1}. Because of the existence of the surface OH groups and the strong H_2 bonding interactions between them, the wide band at approximately 3,463 cm^{-1} is caused. Finally, the band at about 1,637 cm^{-1} can be attributed to the distortion modes of the OH bonds of adsorbed H_2O [35].

3.2. 2-Nitroaniline adsorption

3.2.1. Contact time effect

The contact time duration was determined for the 2-nitroaniline solution to adsorb it onto MCM-48 in order to

attain equilibrium as indicated in Fig. 6. The adsorption of 2-nitroaniline solutions is clearly much influenced by time. The amount adsorbed on the nanoporous material zeolite was quantified for this purpose. The findings showed that equilibrium was established in under 20 min. It may take less time to attain balance. As a result, 60 min was specified to be the ideal contact time for the adsorbent. So, for the MCM-48 adsorbent to get saturated with analysis, just a very little contact time is needed. The adsorption capacity was greatly increased by higher cationic surfactant concentrations and their high availability in the pores of the adsorbent. This finding is significant, since one of the key factors taken into account for an efficient system of wastewater treatment is the equilibrium time. Therefore, in all experiments, adsorption was let to continue for 1 h [36].

3.2.2. Agitation speed effect

The adsorption of hazardous solutes was examined by changing the agitation velocity speed from 0 to 200 rpm while maintaining a concentrated solution and contact time constant. The removal of harmful 2-nitroaniline solutions rose when the agitation velocity was raised from 0 to 150 rpm; however, it then remained constant. This suggests that an agitation velocity in the 150–200 rpm range is enough to ensure the surfactants optimum cationic sites present in the pores of MCM-48 adsorbent are rapidly made available for absorption. The best agitation speed for the remaining studies was determined to be 150 rpm [37].

3.2.3. Concentration effect

As a 2-nitroaniline initial concentration function C_o, Fig. 7 depicts the % removal of 2-nitroaniline estimated from Eq. (1). Approximately 51% of the 2-nitroaniline content, which was initially 4 mg/dm^3, is removed from solution. The % removal of 2-nitroaniline was decreased with the increased concentration at a constant mass of MCM-48. This reduces the amount of concentrated solution material that gradually absorbs more material. The quantity that may adsorb into the pores decreases when the maximum absorption of the MCM-48 pores is approached [38].

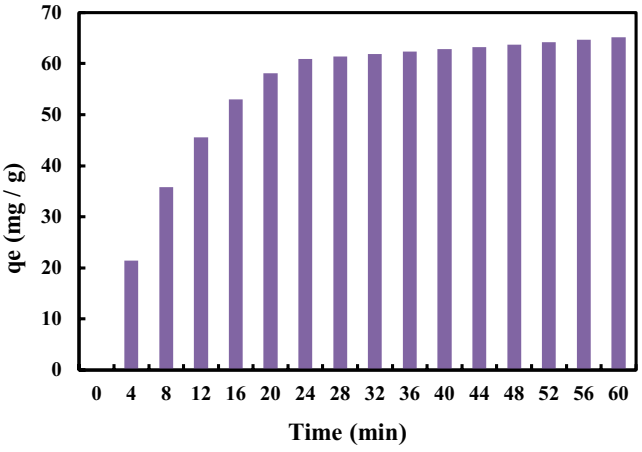

Fig. 6. Contact time effect on the 2-nitroaniline adsorption.

3.3. Adsorption isotherm

Fig. 8 depicts the 2-nitroaniline compound's adsorption isotherms, where C_e represents the adsorbate equilibrium concentration in solution at equilibrium and q_e represents the quantity of adsorbate adsorbed per gram of MCM-48. 2-Nitroaniline molecule was generally adsorbed throughout a variety of concentrations, demonstrating the efficiency of MCM-48 in the removal of 2-nitroaniline from aqueous solutions as an adsorbent. An essential driving factor for overcoming all ion and molecule mass transfer resistances between the solid phases and aqueous is the initial adsorbate concentration [39]. The initial solution concentration in the current investigation is adjusted from 4–60 mg/L however, the adsorbent dose stays constant at 0.01 g/100 mL. Fig. 8 shows that when the equilibrium adsorption capacity increases, the initial 2-nitroaniline concentration also rises. The uptake of equilibrium adsorption for 2-nitroaniline rose from 19–65 mg/g as the starting concentration of 2-nitroaniline aqueous solution increased from 4 to 60 mg/L. This is because of the excess in number of 2-nitroaniline molecules of poisonous solutes vying for the few remaining sites of binding onto the adsorbent's surface. According to the finding shown in Fig. 8, cationic surfactants that include

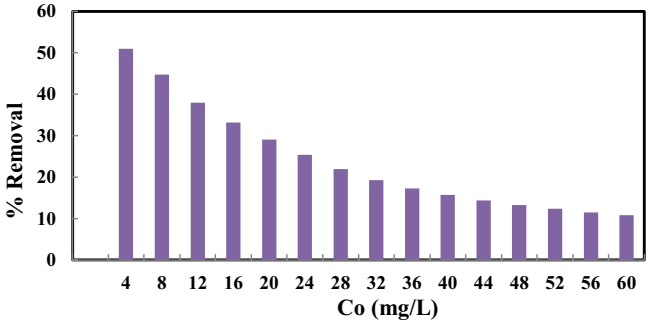

Fig. 7. Initial 2-nitroaniline concentration impact on removal efficiency at contact time = 60 min and MCM-48 dosage = 0.01 g.

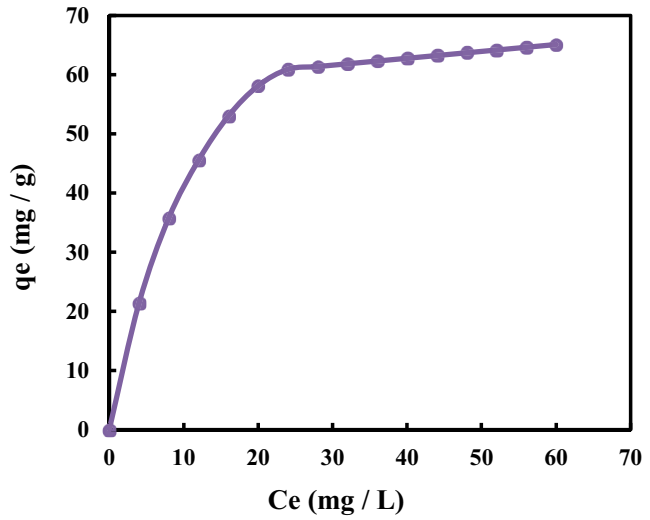

Fig. 8. Adsorption isotherms on MCM-48 with 0.01 g/100 mL adsorbent

MCM-48 have a very high uptake for 2-nitroaniline adsorption. As seen in Fig. 5, silanol groups (Si–OH) constitute significant sites of adsorption on the MCM-48 surface. These sites are present in this substance in addition to cationic sites that were provided by a cationic template. It appears that a key determinant in the adsorption of 2-nitroaniline on the surface of MCM-48 is the number of sorption sites. This can be explained by the fact that there are initially lots of empty surface sites accessible for adsorption. It was also proposed that as time went on, a potent attraction force developed between the molecules of 2-nitroaniline and the sorbent. Due to saturation, it is difficult to fill the remaining open surface sites, which may also be related to a lack of accessible sorption sites towards the conclusion of the adsorption process [40].

The adsorption isotherms for 2-nitroaniline compound have profiles that are consistent with type I Langmuir adsorption; the quantity adsorbed rose gradually until it reached values in the 21–65 mg/g range [41]. The study of adsorption isotherms has been done so as to model the adsorption behavior. According to Figs. 9 and 10, the Freundlich and Langmuir isotherm models were used to assess the 2-nitroaniline species adsorption process. Langmuir and Freundlich equations are given in Eqs. (3) and (4), respectively.

$$\frac{C_e}{q_e} = \left(\frac{1}{bq_{\max}}\right) + \left(\frac{1}{q_{\max}}\right) C_e \tag{3}$$

$$\log q_e = \log K_F + \left(\frac{1}{n}\right) \log C_e \tag{4}$$

Graphing Eq. (3) linear form of, or C_e/q_e vs. C_e, which was applied to determine the constants of Langmuir and maximal uptake or capacity q_{max}, corroborated type I adsorption. According to Table 2 and Fig. 9, the Langmuir profile for the 2-nitroaniline molecule is a straight line, supporting type I adsorption. R^2 values are 0.99. Fig. 9 displays the linearized isotherm data using the Langmuir equation. Table 2 lists the regression coefficients. R^2 = 0.99, a high correlation coefficient, denotes strong agreement between the parameters. 2-Nitroaniline has an adsorption ability to create monolayers that may reach up to 100 mg/g, according to the constant q_{max}. The value of the adsorption energy constant, b, for 2-nitroaniline is 0.5 dm^3/mg. The Freundlich equation was also fitted to the similar data, which is seen in Fig. 10. Table 2 provides the constants of regression. The correlation coefficient values demonstrate how closely the data follow the Langmuir equation. The 2-nitroaniline component adsorption on mesoporous materials is better depicted by the Langmuir model than by the Freundlich model. Furthermore, 2-nitroaniline has 1/n values that are smaller than 1, which is a sign of a high adsorption intensity [42].

3.4. Adsorption kinetics

One of the most important elements that defines the effectiveness of adsorption is the rate of 2-nitroaniline adsorption by MCM-48. A pseudo-first-order and pseudo-second-order model have been applied to explain kinetics of 2-nitroaniline adsorption. Figs. 11 and 12 illustrate how pseudo-first-order and pseudo-second-order kinetics models were used to analyze the 2-nitroaniline kinetics of adsorption onto MCM-48. Table 3 contains the results for

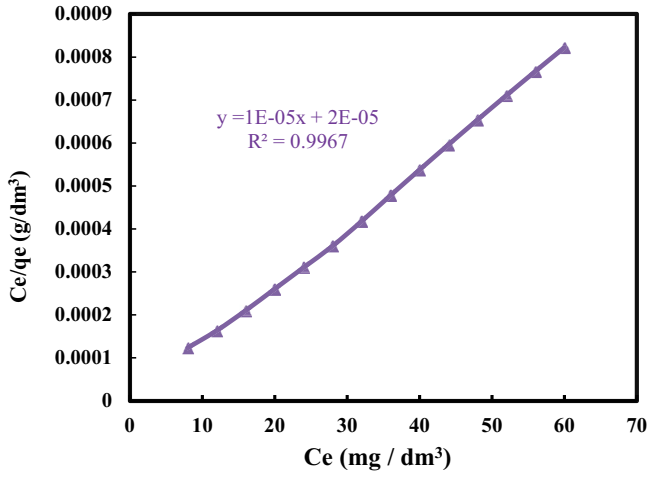

Fig. 9. 2-Nitroaniline adsorption on MCM-48 according to Langmuir isotherms.

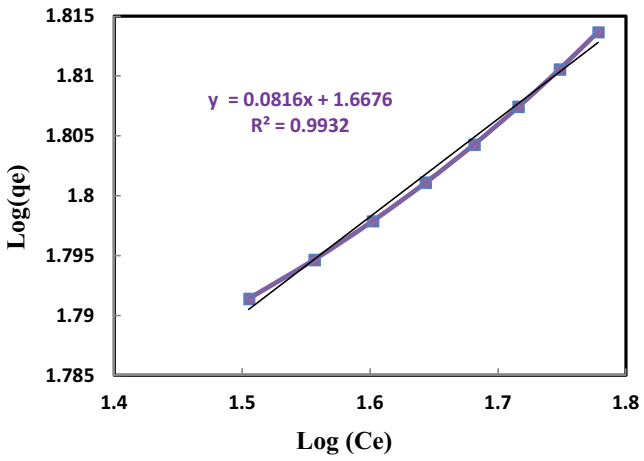

Fig. 10. Freundlich isotherms for the 2-nitroaniline adsorption on MCM-48.

Table 2
Constant of Langmuir and Freundlich for 2-nitroaniline adsorption on MCM-48

Adsorbate	q_{max} (mg/g)	Langmuir constants			Freundlich constants	
		b (dm^3/mg)	R^2	K_F	1/n	R^2
2-Nitroaniline	100	0.5	0.9967	46.515	0.0816	0.9932

the kinetic model parameters and the correlation coefficients (R^2). According to Table 3, the theoretical values ($q_{e,cal}$) calculated from the pseudo-first-order kinetic model gave substantially different values when compared to experimental values ($q_{e,exp}$). As a result, the pseudo-first-order kinetic model is representing this adsorption system well. The theoretical values ($q_{e,cal}$) calculated using the pseudo-second-order kinetic model are extremely close to the experimental values ($q_{e,exp}$), as shown in Table 3. The coefficients R^2 value is also quite near to 1, which supports the validity of the pseudo-second-order equation. In the current research, the adsorption data were analyzed applying two important kinetic models. The integrated pseudo-first-order rate equation is written as [43]:

$$\log\left(q_e - q_t\right) = \log q_e - k_1 t \tag{5}$$

The adsorbed 2-nitroaniline quantity at equilibrium time t is shown by q_e and q_t, respectively. k_1: is the pseudo-first-order adsorption equilibrium rate constant. The pseudo-second-order equation is [44]:

$$\frac{t}{q_t} = \frac{1}{k_2 q_e^2} + \frac{1}{q_e} t \tag{6}$$

where k_2: is the rate constant of pseudo-second-order.

Figs. 11 and 12 explain the findings of pseudo-first-order and pseudo-second-order models were used to fit the experimental data, respectively. The results from the adsorption kinetics are extremely well matched by the pseudo-second-order model, as shown in Fig. 12. Given that 2-nitroaniline regression coefficients are so high (0.98), the pseudo-second-order hypothesis for the adsorption mechanism process appears to be well-supported [45].

3.5. Adsorption mechanism

To understand the adsorption mechanism process, it is important to know the structure of the adsorbent and adsorbate as shown in Fig. 13. 2-Nitroaniline molecule is an organic chemical substance, particularly a primary aromatic amine. It consists of an amino group attached to a benzene ring. On the other hand, MCM-48 adsorbent is the most common molecular sieves of mesoporous materials that is intensively investigated by researchers. The most notable feature of the MCM-48 is that despite having an amorphous silica wall, it has a long-range organized structure and consistent mesoporous. This important material has the majority of silanol group. Based on the structure of the 2-nitroaniline, MCM-48 and experimental results of kinetic, FTIR and EDAX analysis, the adsorption mechanism of 2-nitroaniline onto MCM-48 adsorbent can be determined. Based on FTIR results, the strong adsorption band of at – C=C–group was decreased in intensity and shifted from 1,681 to 1,600 cm^{-1} owing to π–π interactions between 2-nitroaniline molecule with – C=C–onto the surface of MCM-48. While the band of – OH groups was increased in intensity and a slight shift from 3,330 to 3,335 owing to hydrogen bond formation between the – $N(CH_3)_2$ group of 2-nitroaniline molecules and the – OH group in the MCM-48 surface. The band of C=O stretch

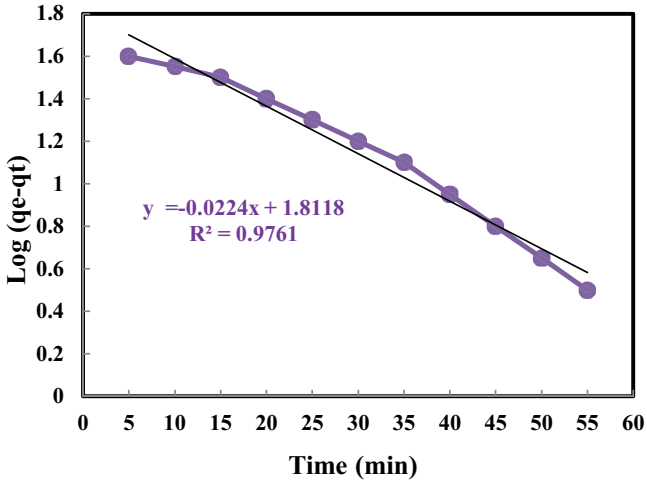

Fig. 11. Pseudo-first-order kinetics for the 2-nitroaniline adsorption on MCM-48.

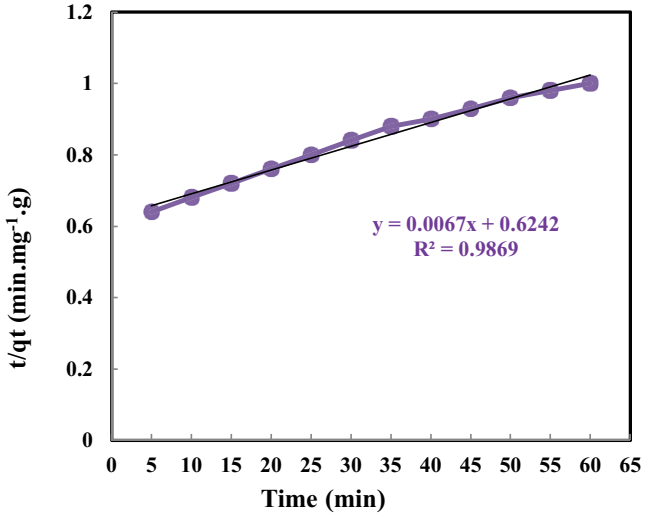

Fig. 12. Pseudo-second-order kinetics for the 2-nitroaniline adsorption on MCM-48.

Table 3
Pseudo-first-order and pseudo-second-order constants for 2-nitroaniline adsorption on MCM-48

Adsorbates	$q_{e,exp}$ (mg/g)	Pseudo-first-order constants			Pseudo-second-order constants		
		$q_{e,cal}$ (mg/g)	k_1 (g/mg·min)	R^2	$q_{e,cal}$ (mg/g)	k_2 (g/mg·min)	R^2
2-Nitroaniline	50	65	0.0224	0.976	149	7.1916×10^{-5}	0.986

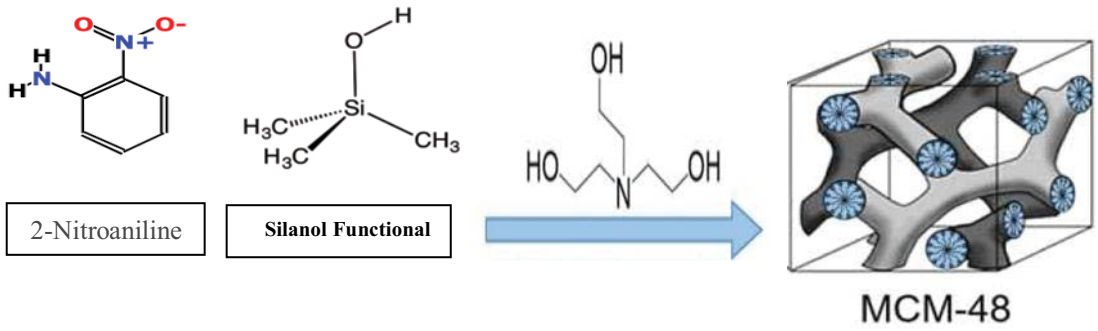

Fig. 13. Mechanism adsorption of 2-nitroaniline onto MCM-48 adsorbent.

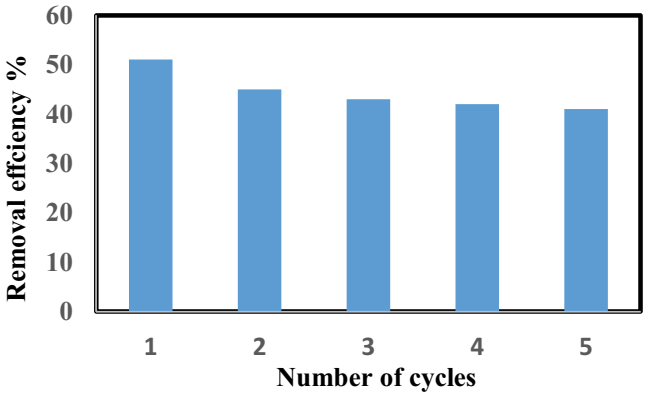

Fig. 14. Reusability of MCM-48 in batch experiment.

vibration of carboxylic acid was a slight increase in intensity due to electrostatic attraction between a cationic $^{+}N(CH_3)_3^{+}$ group of MG molecules with the negative charge of COOH group onto the MCM-48 surface. According to the results of adsorption isotherms and kinetics study, the adsorption mechanism is a chemisorption and physical adsorption process. Therefore, these results provide enough evidence to support the 2-nitroaniline adsorption onto the MCM-48 surface by different mechanisms such as hydrogen bonding, electrostatic interaction and π–π interactions [46–49].

3.6. Adsorbent regeneration

The possibility of recycling the adsorbent in order to reuse it again was examined for applying a depleted MCM-48 after regeneration. For the purpose of proving that the MCM-48 could be regenerate by removing the adsorbates, desorption investigations were carried out. When using the MCM-48 again, it is crucial to establish that desorption takes place. According to the results of the trials, 2-nitroaniline was effectively and efficiently desorbed into deionized water in a single cycle, with an efficiency of over 90%. It can be seen from this that all used materials may be recycled. It is possible to perform a more thorough investigation to learn more about desorption, including the impacts of solution concentration, adsorbate loading, temperature, etc. The focus of this essay does not extend to this [50]. The results of regeneration and recirculation of MCM-48 are shown in Fig. 14. This figure indicates that the removal efficiency of 2-nitroaniline was changed only from 51% to 41% after five regeneration cycles of MCM-48. This means that MCM-48 can be easily reused and regenerated efficiently.

Table 4
Adsorption capacities of 4-nitroaniline by various adsorbents

No.	Adsorbents	Adsorption capacity q_{max} (mg/g)	References
1	Beta zeolite	100	[35]
2	ZSM-5 zeolite	37.2	[37]
3	Activated carbon	383	[51]
4	Mesoporous materials MCM-48	65	This study

3.7. Comparative study

Table 4 compares the MCM-48 with several other adsorbents mentioned in the literature. This table offers important details regarding how effectively MCM-48 adsorbent may increase 2-nitroaniline's capacity for adsorption from other adsorbent materials. Pure MCM-48 has an adsorption capability of 65 mg/g for 2-nitroaniline without functionalization or treatment of its surface. One may conclude that adding a functional group to the surface of MCM-48 will increase its adsorption capacity. Table 4 shows that MCM-48 is a superior adsorbent for removing 2-nitroaniline dye because it has a higher surface area than the other adsorbents, reaching 1,350 m^2/g.

4. Conclusion

In this study, 2-nitroaniline was easily adsorbed from an aqueous adsorbate solution utilizing from the MCM-48 mesoporous material. According to a linear analysis with R^2 values of 0.99, 2-nitroaniline molecules matched to type I Langmuir adsorption. Under appropriate experimental circumstances, nanoporous material demonstrated considerable aniline adsorption capacity; as a result, it may be suggested as a practical adsorbent. The Langmuir adsorption isotherm was discovered the best suited with the experimental, indicating monolayer adsorption on a homogeneous surface. The Langmuir isotherm was used

to calculate the theoretical and experimental maximal adsorption capacity of 100 and 65 mg/g, respectively. The pseudo-second-order model can forecast the dynamics of adsorption. Adsorption isotherms and kinetics models indicate that chemical and physical adsorption are the two processes involved in the adsorption mechanism.

Acknowledgments

The authors are grateful to the Department of Chemical Engineering at the University of Technology-Iraq, the Mustansiriyah University/College of Engineering/Materials Engineering Department Baghdad-Iraq, the Department of Chemical and Petroleum Industries Engineering, Al-Mustaqbal University College, Babylon, Iraq.

Declarations

Ethics approval and consent to participate

Not applicable.

Competing interests

The authors declare that they have no competing interests.

Consent for publication

Not applicable.

Funding

Not Applicable.

Availability of data and material

All relevant data and material are presented in the main paper.

References

[1] A. Al-Nayili, H. Sh. Majdi, T.M. Albayati, N.M. Cata Saady, Formic acid dehydrogenation using noble-metal nanoheterogeneous catalysts: towards sustainable hydrogen-based energy, Catalysts, 12 (2022) 324, doi: 10.3390/catal12030324.
[2] S.M. Alardhi, J.M. Alrubaye, T.M. Albayati, Removal of methyl green dye from simulated wastewater using hollow fiber ultrafiltration membrane, IOP Conf. Ser.: Mater. Sci. Eng., 928 (2020) 052020, doi: 10.1088/1757-899X/928/5/052020.
[3] J. O'Brien, T.F. O'Dwyer, T. Curtin, A novel process for the removal of aniline from wastewaters, J. Hazard. Mater., 159 (2008) 476–482.
[4] E.H. Khader, R.H. Khudhur, N.S. Abbood, T.M. Albayati, Decolourisation of anionic azo dye in industrial wastewater using adsorption process: investigating operating parameters, Environ. Processes, 10 (2023) 34, doi: 10.1007/s40710-023-00646-7.
[5] C. Ko, S. Chen, Enhanced removal of three phenols by lactase polymerization with MF/UF membranes, Bioresour. Technol., 99 (2008) 2293–2298.
[6] N.S. Ali, K.R. Kalash, A.N. Ahmed, T.M. Albayati, Performance of a solar photocatalysis reactor as pretreatment for wastewater via UV, UV/TiO_2, and UV/H_2O_2 to control membrane fouling, Sci. Rep., 12 (2022) 16782, doi: 10.1038/s41598-022-20984-0.
[7] N.S. Abbood, N.S. Ali, E.H. Khader, H. Sh. Majdi, T.M. Albayati, N.M. Cata Saady, Photocatalytic degradation of cefotaxime pharmaceutical compounds onto a modified nanocatalyst, Res. Chem. Intermed., 49 (2023) 43–56.
[8] A.L. Ahmad, K.Y. Tan, Reverse osmosis of binary organic solute mixtures in the presence of strong solute-membrane affinity, Desalination, 165 (2004) 193–199.
[9] V.V. Goncharuk, D.D. Kucheruk, V.M. Kochkodan, V.P. Badekha, Removal of organic substances from aqueous solutions by reagent enhanced reverse osmosis, Desalination, 143 (2002) 45–51.
[10] T. Hirakawa, T. Daimon, M. Kitazawa, N. Ohguri, C. Koga, N. Negishi, S. Matsuzawa, Y. Nosaka, An approach to estimating photocatalytic activity of TiO_2 suspension by monitoring dissolved oxygen and superoxide ion on decomposing organic compounds, J. Photochem. Photobiol., A, 190 (2007) 58–68.
[11] A.M. Amat, A. Arques, M.A. Miranda, S. Seguí, R.F. Vercher, Degradation of rosolic acid by advanced oxidation processes: ozonation vs. solar photocatalysis, Desalination, 212 (2007) 114–122.
[12] G.L. Puma, P.L. Yue, Effect of the radiation wavelength on the rate of photocatalytic oxidation of organic pollutants, Ind. Eng. Chem. Res., 41 (2002) 5594–5600.
[13] N.M. Al-Bastaki, Performance of advanced methods for treatment of wastewater: UV/TiO_2, RO and UF, Chem. Eng. Process. Process Intensif., 43 (2004) 935–940.
[14] R. Morent, J. Dewulf, N. Steenhaut, C. Leys, H. Van Lagenhove, Hybrid plasma catalyst system for the removal of trichloroethylene from air, J. Adv. Oxid. Technol., 9 (2006) 53–58.
[15] J. Levec, A. Pintar, Catalytic wet-air oxidation processes: a review, Catal. Today, 124 (2007) 172–184.
[16] S.K. Bhargava, J. Tardio, H. Jani, D.D. Akolekar, K. Foeger, M. Hoang, Catalytic wet-air oxidation of industrial waste streams, Catal. Surv. Asia, 11 (2007) 70–86.
[17] C.H. Ko, C. Fan, P.N. Chiang, M.K. Wang, K.C. Lin, *p*-Nitrophenol, phenol and aniline sorption by organo-clays, J. Hazard. Mater., 149 (2007) 275–282.
[18] S. Razee, T. Masujima, Uptake monitoring of anilines and phenols using modified zeolites, Anal. Chim. Acta, 464 (2002) 1–5.
[19] M. Khalid, G. Joly, A. Renaud, P. Magnoux, Removal of phenol from water by adsorption using zeolites, Ind. Eng. Chem. Res., 43 (2004) 5275–5280.
[20] N.M. Milestone, D.M. Bibby, Concentration of alcohols by adsorption on silicalite, J. Chem. Technol. Biotechnol., 31 (1981) 732–736.
[21] E. Narita, N. Horiguchi, T. Okabe, Adsorption of phenols, cresols and benzyl alcohol from aqueous solution by silicalite, Chem. Lett., 6 (1985) 787–790.
[22] U.S. Taralkar, M.W. Kasture, P.N. Joshi, Influence of synthesis condition on structure properties of MCM-48, J. Phys. Chem. Solids, 69 (2008) 2075–2081.
[23] L. Pajchel, W. Kolodziejski, Synthesis and characterization of MCM 48/hydroxyapatite composites for drug delivery: ibuprofen incorporation, location and release studies, Mater. Sci. Eng., C, 91 (2018) 734–742.
[24] M. Shaban, M.R. Abukhadra, A. Hamd, R. Amin, A. Khalek, Photocatalytic removal of Congo red dye using MCM-48/Ni_2O_3 composite synthesized based on silica gel extracted from rice husk ash; fabrication and application, J. Environ. Manage., 204 (2017) 189–199.
[25] R. Nejat, A.R. Mahjoub, Z. Hekmatian, A. Tahereh, Pd-functionalized MCM-41 nanoporous silica as an efficient and reusable catalyst for promoting organic reactions, RSC Adv., 5 (2015) 16029–16035.
[26] A.M. Doyle, B.K. Hodnett, Synthesis of 2-cyanoethyl-modified MCM-48 stable to surfactant removal by solvent extraction: influence of organic modifier, base and surfactant, Microporous Mesoporous Mater., 58 (2003) 255–261.
[27] A.M. Doyle, E. Ahmed, B.K. Hodnett, The evolution of phases during the synthesis of the organically modified catalyst support MCM-48, Catal. Today, 116 (2006) 50–55.

[28] T.M. Albayati, A.M. Doyle, SBA-15 supported bimetallic catalysts for enhancement isomers production during *n*-heptane decomposition, Int. J. Chem. Reactor Eng., 12 (2014) 345–354.
[29] T.M. Albayati, S.E. Wilkinson, A.A. Garforth, A.M. Doyle, Heterogeneous alkane reactions over nanoporous catalysts, Transp. Porous Media, 104 (2014) 315–333.
[30] T.M. Albayati, A.A. Sabri, D.B. Abed, Functionalized SBA-15 by amine group for removal of Ni(II) heavy metal ion in the batch adsorption system, Desal. Water Treat., 174 (2020) 301–310.
[31] W.A. Muslim, T.M. Albayati, S.K. Al-Nasri, Decontamination of actual radioactive wastewater containing ^{137}Cs using bentonite as a natural adsorbent: equilibrium, kinetics, and thermodynamic studies, Sci. Rep., 12 (2022) 13837, doi: 10.1038/s41598-022-18202-y.
[32] Y.A. Abd Al-Khodor, T.M. Albayati, Real heavy crude oil desulfurization onto nanoporous activated carbon implementing batch adsorption process: equilibrium, kinetics, and thermodynamic studies, Chem. Afr., 6 (2023) 747–756.
[33] S. Han, J. Xu, W. Hou, X. Yu, Y. Wang, Synthesis of high-quality MCM-48 mesoporous silica using Gemini surfactant dimethylene-1,2-bis(dodecyldimethylammonium bromide), J. Phys. Chem. B, 108 (2004) 15043–15048.
[34] Z. Qiang, X. Bao, W. Ben, MCM-48 modified magnetic mesoporous nanocomposite as an attractive adsorbent for the removal of sulfamethazine from water, Water Res., 47 (2013) 4107–4114.
[35] T.M. Al-Bayati, Removal of aniline and nitro-substituted aniline from wastewater by particulate nanoporous MCM-48, Part. Sci. Technol., 32 (2014) 616–623.
[36] H. Tian, J. Li, L. Zou, Z. Mua, Z. Hao, Removal of DDT from aqueous solutions using mesoporous silica materials, J. Chem. Technol. Biotechnol., 84 (2009) 490–496.
[37] T.M. Albayati, A.M. Doyle, Purification of aniline and nitrosubstituted aniline contaminants from aqueous solution using beta zeolite, Chem.: Bulg. J. Sci. Educ., 23 (2014) 105–114.
[38] S. Fauzia, H. Aziz, D. Dahlan, R. Zein, Study of equilibrium, kinetic and thermodynamic for removal of Pb(II) in aqueous solution using Sago bark (*Metroxylon sago*), AIP Conf. Proc., 2023 (2018) 020081, doi: 10.1063/1.5064078.
[39] T.M. Albayati, A.M. Doyle, Shape-selective adsorption of substituted aniline pollutants from wastewater, Adsorpt. Sci. Technol., 31 (2013) 459–468.
[40] L. Bois, A. Bonhommé, A. Ribes, B. Pais, G. Raffin, F. Tessier, Functionalized silica for heavy metal ions adsorption, Colloids Surf., A, 221 (2003) 221–230.
[41] R. Saad, K. Belkacemi, S. Hamoudi, Adsorption of phosphate and nitrate anions on ammonium-functionalized MCM-48: effects of experimental conditions, J. Colloid Interface Sci., 311 (2007) 375–381.
[42] A.T. Khadim, T.M. Albayati, N.M. Cata Saady, Desulfurization of actual diesel fuel onto modified mesoporous material Co/MCM-41, Environ. Nanotechnol. Monit. Manage., 17 (2022) 100635, doi: 10.1016/j.enmm.2021.100635.
[43] S.T. Kadhum, G.Y. Alkindi, T.M. Albayati, Remediation of phenolic wastewater implementing nano zerovalent iron as a granular third electrode in an electrochemical reactor, Int. J. Environ. Sci. Technol., 19 (2022) 1383–1392.
[44] S.T. Kadhum, G.Y. Alkindi, T.M. Albayati, Determination of chemical oxygen demand for phenolic compounds from oil refinery wastewater implementing different methods, Desal. Water Treat., 231 (2021) 44–53.
[45] N.S. Ali, N.M. Jabbar, S.M. Alardhi, H. Sh. Majdi, T.M. Albayati, Adsorption of methyl violet dye onto a prepared bio-adsorbent from date seeds: isotherm, kinetics, and thermodynamic studies, Heliyon, 8 (2022) e10276, doi: 10.1016/j.heliyon.2022.e10276.
[46] A. Amari, H.S.K. Alawamleh, M. Isam, M.A.J. Maktoof, H. Osman, B. Panneerselvam, M. Thomas, Thermodynamic investigation and study of kinetics and mass transfer mechanisms of oily wastewater adsorption on UIO-66-$MnFe_2O_4$ as a metal–organic framework (MOF), Sustainability, 15 (2023) 2488, doi: 10.3390/su15032488.
[47] A.Q. Alorabi, M. Azizi, Effective removal of methyl green from aqueous environment using activated residual *Dodonaea Viscosa*: equilibrium, isotherm, and mechanism studies, Environ. *Pollut. Bioavailability*, 35 (2023) 2168761, doi: 10.1080/26395940.2023.2168761.
[48] L.D. Duceac, E. Tarca, M.I. Ciuhodaru, M.M. Tantu, R.E.B. Goroftei, E.A. Banu, D. Damir, M. Glod, A.C. Luca, Study on the mechanism of antibiotic resistance, Rev. Chim., 70 (2019) 199–201.
[49] A.C. Luca, L.D. Duceac, G. Mitrea, M.I. Ciuhodaru, D.L. Ichim, G. Baciu, E.A. Banu, A.C. Iordache, Antibiotic encapsulated nanomaterials with application in medical area, Mater. Plast., 55 (2018) 552–554.
[50] H.J. Al-Jaaf, N.S. Ali, S.M. Alardhi, T.M. Albayati, Implementing eggplant peels as an efficient bio-adsorbent for treatment of oily domestic wastewater, Desal. Water Treat., 245 (2022) 226–237.
[51] K. Li, Z. Zheng, X. Huang, G. Zhao, J. Feng, J. Zhang, Equilibrium, kinetic and thermodynamic studies on the adsorption of 2-nitroaniline onto activated carbon prepared from cotton stalk fibre, J. Hazard. Mater., 166 (2009) 213–220.